Published in final edited form as:
Neuroimage. 2010 February 1; 49(3): 2311. doi:10.1016/j.neuroimage.2009.10.040.

Caffeine Increases the Linearity of the Visual BOLD Response

Thomas T. Liu and **Joy Liau**
Center for Functional Magnetic Resonance Imaging and Departments of Radiology and Bioengineering, University of California San Diego, La Jolla, CA

Abstract

Although the blood oxygenation level dependent (BOLD) signal used in most functional magnetic resonance imaging (fMRI) studies has been shown to exhibit nonlinear characteristics, most analyses assume that the BOLD signal responds in a linear fashion to stimulus. This assumption of linearity can lead to errors in the estimation of the BOLD response, especially for rapid event-related fMRI studies. In this study, we used a rapid event-related design and Volterra kernel analysis to assess the effect of a 200 mg oral dose of caffeine on the linearity of the visual BOLD response. The caffeine dose significantly ($p < 0.02$) increased the linearity of the BOLD response in a sample of 11 healthy volunteers studied on a 3 Tesla MRI system. In addition, the agreement between nonlinear and linear estimates of the hemodynamic response function was significantly increased ($p= 0.013$) with the caffeine dose. These findings indicate that differences in caffeine usage should be considered as a potential source of bias in the analysis of rapid event-related fMRI studies.

Introduction

Functional magnetic resonance imaging (fMRI) is a widely used technique for the non-invasive mapping and measurement of brain function in both normal subjects and clinical populations. Most fMRI studies rely on the blood oxygenation level dependent (BOLD) signal, which is a complex function of changes in neural activity, oxygen metabolism, cerebral blood volume, cerebral blood flow (CBF), and other physiological parameters (Buxton et al. 2004). Although the link between neural activity and the BOLD response is not completely understood, fMRI studies typically treat the BOLD response as an indirect measure of neural activity. In particular, most analyses of BOLD fMRI studies assume that the BOLD response to stimulus can be modeled using a linear time invariant system (Boynton et al. 1996). Although the assumption of linearity greatly simplifies the analysis process, a number of studies have now shown that there are significant nonlinearities in the BOLD response (Dale and Buckner 1997; Friston et al. 1998; Vasquez and Noll 1998; Glover 1999; Huettel and McCarthy 2000; Birn et al. 2001; Wager et al. 2005). Consideration of these nonlinearities is especially important for rapid event-related experimental designs, in which varying stimuli are presented at a rapid pace. Event-related experimental designs are now widely used for cognitive studies because of their ability to reduce psychological confounds such as anticipation and habituation (Rosen et al. 1998). Because the close temporal spacing between stimuli can result in nonlinear

Correspondence to: Thomas T. Liu, Ph.D., UCSD Center for Functional MRI, 9500 Gilman Drive, MC 0677, La Jolla, CA 92093-0677, Phone: 858-822-0542, FAX: 858-822-0605, ttliu@ucsd.edu.

interactions, a linear analysis of a rapid event-related design can result in reduced sensitivity and errors in the estimates of response amplitudes (Wager et al. 2005).

Prior work examining the linearity of the BOLD response has been focused primarily on healthy young control subjects. In this work, we consider how changes in the baseline vascular state can alter the linearity of the BOLD response. This line of research is motivated by growing evidence that changes in the baseline vascular state, due to factors such as medication and age, can greatly alter the dynamics of the BOLD signal (D'Esposito et al. 1999). For example, vasodilation due to hypercapnia (increased carbon dioxide) has been shown to increase the temporal width and decrease the amplitude of the BOLD hemodynamic response (HRF), while vasoconstriction caused by hypocapnia has the opposite effect (Kemna and Posse 2001; Cohen et al. 2002). The effects of caffeine and hyperoxia, both of which are vasoconstrictive agents, have been shown to be similar to those observed with hypocapnia (Kashikura et al. 2000; Liu et al. 2004). Several studies have reported age-related increases in temporal parameters (e.g. latency and time-to-peak) (Taoka et al. 1998; Mehagnoul-Schipper et al. 2002; Richter and Richter 2003), and decreases in amplitude (Ross et al. 1997; Buckner et al. 2000; Hesselmann et al. 2001), while other studies have found conflicting results (D'Esposito et al. 1999; Huettel et al. 2001). These changes may reflect normal age-related reduction in vessel elasticity or vascular remodeling in response to the onset and progression of atherosclerosis and hypertension with age (Farkas and Luiten 2001; Liao et al. 2004; Izzard et al. 2005).

In an effort to explain the effects of vasoactive agents and age on the dynamics of the BOLD response, (Behzadi and Liu 2005) introduced a theoretical model called the arteriolar compliance model. Using their model, they showed that modulations of the baseline vascular state, such as an increase in CBF with hypercapnia, could alter the responsiveness of the arterioles and thereby change the amplitude and shape of the BOLD response. The dynamics of the model exhibit a strong dependence on the baseline state of the arteriole, reflecting the fact that the arteriolar wall consists of an active element (vascular smooth muscle) and a passive element (collagen and basement membrane), where the stress taken up by the passive element increases exponentially with radius. This two-element model results in a nonlinear relation between radius and muscular compliance. In the presence of an externally applied vasodilatory agent, such as carbon dioxide, the smooth muscle relaxes and exerts less force so that the vessel may expand, while the less compliant passive element becomes stiffer as the radius increases, in a manner similar to the walls of a rubber tube becoming stiffer as it expands. Within the framework of the model, the increased stiffness of the passive element causes the arteriole to operate in a more nonlinear regime, leading to a reduction in vascular responsiveness and a slowing down of the BOLD response. In contrast, with the application of vasoconstrictive agents, the smooth muscle contracts, and the stress exerted by the passive element lessens as the arteriolar radius decreases. The reduced influence of the passive element allows the arteriole to operating in a more linear regime, resulting in an increase in the responsiveness of the arteriole and a quickening of the BOLD response.

The arguments described above suggest that the linearity of the BOLD response may also depend on the baseline vascular state, with vasoconstriction leading to an increase in linearity and vasodilation leading to a decrease in linearity. In this study, we tested one component of this hypothesis by assessing the effects of caffeine, a vasoconstrictor, on the linearity of the BOLD response.

Methods

Experimental protocol

Eleven healthy adult volunteers (ages 20 to 40 years) participated in the study after giving informed consent. Each subject was asked to refrain from ingesting any food or drink

containing caffeine for at least 12 h before the imaging experiment. The estimated daily caffeine usage of each subject based on self-report of coffee, tea, and caffeinated soda consumption was assessed; the assumed caffeine contents for an 8-oz cup of coffee, an 8-oz cup of tea, and a 12-oz can of soda were 100 mg, 40 mg, and 20 mg, respectively (Fredholm et al. 1999). Eight of the 11 subjects had an estimated caffeine usage of less than 50 mg per day while the remaining 3 had an estimated usage of about 200 mg per day.

Each imaging experiment lasted 2.5 h, consisting of a pre-dose imaging session (60 min), ingestion of a 200 mg dose of caffeine with a 30 min rest period outside of the magnet, and a post-dose imaging session (60 min). This protocol is similar in structure to previously described imaging protocols involving caffeine (Liu et al. 2004; Behzadi and Liu 2006). The first functional scan of the post-dose session started approximately 40 min after the dose. This interval was chosen based on studies showing that the absorption of caffeine from the gastrointestinal tract reaches 99% about 45 min. after ingestion, with a half-life ranging from 2.5 to 4.5 h (Fredholm et al. 1999). During each imaging session, subjects were presented with a visual stimulus consisting of “on” periods of a full-field, full-contrast radial 8-Hz flickering checkerboard with a small white fixation square at the center of the screen and “off” periods of a gray background with the same white fixation square. The average luminance of the off period was equal to the average luminance of the on period. Each imaging session consisted of the following set of functional paradigms: (a) a block design paradigm with a 20-s initial off period followed by four cycles of 20-s on and 40-s off, (b) two repeats of a periodic single trial paradigm with an initial 20-s off period followed by 5 cycles of 4-s on and 40-s off, (c) two repeats of a mixed design paradigm with a 12-s initial off period, followed by two cycles of 1-s on and 20-s off and then 192-s of a random stimulus pattern, and (d) a BOLD resting-state paradigm where the subject was presented with the off condition for 3 min. The random stimulus pattern consisted of 96 events of 1 second duration that were randomly distributed over 192 seconds. Presentation of the periodic single trial and mixed design paradigms was interleaved. The data from the periodic single trial and the BOLD resting-state runs are not analyzed in this paper. In addition, an arterial spin labeling (ASL) resting-state scan, during which the subject was presented with the off condition for 3 min, was performed and used to characterize the resting CBF level.

Image acquisition

Imaging data were acquired on a GE Signa Excite 3 Tesla whole body system with a body transmit coil and an eight channel receive coil. Laser alignment was used to landmark the subjects and minimize differences in head position between pre-dose and post-dose sessions. During the block design paradigm and ASL resting-state scan, data were acquired with a PICORE QUIPSS II (Wong et al. 1998) ASL sequence (TR = 2 s, TI1/TI2 = 600/1500 ms, 10-cm tag thickness, and a 1-cm tag-slice gap) with a dual echo spiral readout (TE1/TE2 = 9.1/30 ms, FOV = 24 cm, 64 × 64 matrix, and a flip angle of 90°). Small bipolar crusher gradients were included to remove signal from large vessels ($b = 2 s/mm^2$). Three oblique axial 8-mm slices were prescribed about the calcarine sulcus for all runs. During the periodic single trial and mixed paradigms, BOLD-weighted images were acquired using a single-shot spiral readout (TE = 25 ms, TR = 500 ms, FOV = 24 cm, 64 × 64 matrix, and a flip angle of 45 degrees). The same parameters were used in the BOLD resting-state paradigm with the exception of TR = 250 ms and flip angle of 40 degrees.

A high-resolution structural scan was acquired with a magnetization prepared 3D fast spoiled gradient echo (FSPGR) sequence (TI = 450 ms, TR = 8.2 ms, TE = 3.1 ms, 12 degree flip angle, FOV 25 × 25 × 25.6 cm, matrix 256 × 256 × 256). In addition, a cerebrospinal fluid (CSF) reference scan and a minimum contrast scan were acquired for use in CBF quantification. The CSF scan consisted of a single-echo, single repetition scan acquired at full relaxation and echo

time equal to 9.1 ms, while the minimum contrast scan was acquired with TR = 2 s and TE = 11 ms. Both scans used the same in-plane parameters as the ASL scans, but the number of slices was increased to cover the lateral ventricles.

Cardiac and respiratory fluctuations were monitored using a pulse oximeter (InVivo MDE, Orlando, FL) and a respiratory effort transducer (BIOPAC Systems Inc., Goleta CA), respectively. The pulse oximeter was placed on the subject's right index finger, and the respiratory effort belt was placed around the subject's abdomen. Physiological data were sampled at 40 samples per second using a multi-channel data acquisition board (National Instruments). Scanner TTL pulse data were sampled at 1000 samples per second by the same data acquisition board to allow synchronization of physiological data to the MRI acquisitions.

Data Preprocessing

Images were co-registered and motion corrected using AFNI software (Cox 1996). The structural scan from each post-dose session was aligned to the structural scan of its respective pre-dose session, and the rotation and shift matrix used for this alignment was then applied to the post-dose BOLD and ASL images (Liu et al. 2004). Data from the first ten seconds of each run were discarded to allow magnetization to reach a steady state.

Definition of Regions of Interest

A joint region of interest (ROI) was used for the analyses of pre-dose and post-dose data. To define this ROI, we first determined a joint region consisting of voxels with at least 90% overlap of volume between the pre-dose and post-dose imaging sessions. We then identified those voxels within the overlap region that exhibited significant functional activation in the ASL block design runs in both the pre-dose and post-dose sessions. A general linear model (GLM) analysis of the first echo and second echo data from the block runs was used to generate statistical maps for the perfusion and BOLD responses, respectively. Cardiac and respiratory data were used as physiological nuisance regressors in the GLM (Restom et al. 2006). The statistical maps were thresholded at an overall significance level of $p = 0.05$, with correction for multiple comparisons using the AFNI AlphaSim program (Forman et al. 1995; Cox 1996). Voxels that were active in both the perfusion and BOLD activation maps across the pre-dose and post-dose sessions were included in the joint ROI.

Baseline CBF

For each subject, a mean ASL image was formed from the average difference of the control and tag images from the first echo of the ASL resting-state scan data (Liu and Wong 2005). This mean ASL image was then corrected for coil inhomogeneities using the minimum contrast image (Wang et al. 2005) and converted to physiological units (ml/(100g-min) of cerebral blood flow (CBF) using the CSF image as a reference signal (Chalela et al. 2000; Liau and Liu 2009). The average baseline CBF within the joint ROI was then computed.

Volterra Kernel Analysis

The linearity of the BOLD responses was accomplished using a Volterra kernel analysis of the data from the mixed design runs. A GLM based approach was used to remove low frequency drift terms (0^{th} through 2^{nd} order Legendre polynomials, corresponding to a constant term, a linear term, and a quadratic term) and physiological noise contributions (Glover et al. 2000; Restom et al. 2006). The data from the mixed runs were then averaged across the two runs and all voxels within the joint ROI. A Volterra kernel analysis was performed for the average time series from the joint ROI.

We used a second-order Volterra kernel model of the form

$$y[n]=\sum_{m=0}^{N_1-1} h_1[m]x[n-m]+\sum_{r=0}^{N_2-1}\sum_{s=0}^{N_2-1} h_2[r,s]x[n-r]x[n-s]+e[n] \quad [1]$$

where $y[n]$ is the measured data, $x[n]$ represents the stimulus, $e[n]$ is additive noise, and $h_1[m]$ and $h_2[r,s]$ are the first and second order kernels, respectively, with the size of the ith order kernel denoted as N_i (Doyle et al. 2002). The first order kernel $h_1[m]$ is analogous to the impulse response of a linear time-invariant system, while the second order kernel $h_2[r,s]$ is used to model second order nonlinearities. For the analysis of fMRI data, it is convenient to rewrite Equation 1 in matrix form as follows:

$$\mathbf{y}=\mathbf{X}_1\mathbf{h}_1+\mathbf{X}_2\mathbf{h}_2+\mathbf{e} \quad [2]$$

where $\mathbf{y}$ is the observed data, $\mathbf{h}_1$ is a column vector representing the first order kernel, $\mathbf{h}_2$ is a column vector with the second order kernel terms, $\mathbf{X}_1$ is the standard linear design matrix whose columns are shifted versions of $x[n]$, $\mathbf{X}_2$ is the second-order design matrix whose columns contain the cross-products $x[n-r]x[n-s]$, and $\mathbf{e}$ is additive noise.

In this paper, the stimulus $x[n]$ is modeled as a binary sequence consisting of 0's and 1's. As a result, $\mathbf{X}_1$ and $\mathbf{X}_2$ are not linearly independent since $x[i]=x[i]x[i]$, and it is not possible to estimate the kernel coefficients. In general, it has been shown that a $(p+1)$-level excitation sequence is required to characterize a pth order Volterra system without ambiguity (Nowak and Van Veen 1994). The matrices $\mathbf{X}_1$ and $\mathbf{X}_2$ can be made linearly independent by removing columns consisting of products $x[r]x[r]$ of repeated indices from $\mathbf{X}_2$. This is equivalent to only estimating the off-diagonal ($r \neq s$) terms of the second order kernel $h_2[r,s]$. The estimate of $\mathbf{h}_1$ then reflects the sum $h_1[m]+h_2[m,m]$ of the first order kernel and the diagonal terms of the second order kernel. The impulse response of a second order Volterra system is also $h_1[m]+h_2[m,m]$, so that the estimate of $\mathbf{h}_1$ is equivalent to a linear estimate of the HRF obtained from an experiment with minimal nonlinear interactions, e.g. a periodic single trial design with widely spaced stimuli. In addition, the estimate of $\mathbf{h}_2$ only includes the off-diagonal terms of the second order kernel. With these restrictions in mind, we will refer to $\mathbf{h}_1$ and $\mathbf{h}_2$ as the first and second order kernel estimates for the remainder of the paper.

For the least squares estimation of the kernels $\mathbf{h}_1$ and $\mathbf{h}_2$ in Equation 2, we assumed kernel sizes of $N_1=30$ (corresponding to a 30 second long hemodynamic response) and $N_2=15$, which models nonlinear interactions up to a lag of 14 seconds. Examples of kernel estimates are shown in Figure 1. Note that for display of the second order kernel $h_2[r,s]$, the elements of the column vector $\mathbf{h}_2$ are arranged as a two dimensional matrix with zeroes along the diagonal (since these terms cannot be estimated).

Metrics of Linearity

We constructed various metrics to assess linearity. Three of these metrics are defined using the ratios of the "size" of the first order kernel $\mathbf{h}_1$ to the "size" of the second order kernel $\mathbf{h}_2$. These are the first three metrics (labeled k_1, k_2, and k_∞) shown in Table 1 and utilize the L_1 norm, the L_2 norm, and the maximum absolute value (L_∞) norm as measures of size, respectively (Golub and Loan 1989). As a system becomes more linear, the size of the first order kernel increases relative to the size of the second order kernel, so that each of these metrics also increases.

In addition to the kernel-based metrics, we also defined linearity metrics based on estimates of the linear and nonlinear components of the response. Towards that end, we defined the linear component of the response as

$$\mathbf{y}_{LIN}=\mathbf{X}_1\widehat{\mathbf{h}}_1, \quad [3]$$

a nonlinear component as

$$\mathbf{y}_{NONLIN}=\mathbf{X}_2\widehat{\mathbf{h}}_2, \quad [4]$$

and the full model response as the sum of the linear and nonlinear components

$$\mathbf{y}_{FULL}=\mathbf{y}_{LIN}+\mathbf{y}_{NOLIN}=\mathbf{X}_1\widehat{\mathbf{h}}_1+\mathbf{X}_2\widehat{\mathbf{h}}_2 \quad [5]$$

where the circumflex indicates that we are using the estimated kernels. Examples of these responses are shown in Figure 1. From these components, we defined two additional metrics (labeled l_1 and l_2 in Table 1) based on the ratios of the size of the linear component to the nonlinear component, after removal of the mean for each component. As a system becomes more linear, the relative size of the linear component increases and the metrics will tend to get larger. In addition, we defined a metric $r_{LIN,FULL}$ as the correlation coefficient between $\mathbf{y}_{LIN}$ and $\mathbf{y}_{FULL}$. This metric is equal to 1 for a completely linear system and decreases in value as the system becomes more nonlinear. To test the hypothesis that caffeine increases the linearity of the BOLD response, we used two-tailed paired t-tests to compare the pre-dose and post-dose linearity metrics.

Linear Estimates of the Hemodynamic Response Function

When using the Volterra signal model in Equation 2, an estimate of the first order kernel $\mathbf{h}_1$ serves as an estimate of the hemodynamic response function. However, because of the added complexity and lower statistical efficiency of Volterra kernel analyses, most event-related fMRI studies use a linear analysis of the data, with a signal model of the form

$$\mathbf{y}=\mathbf{X}_1\mathbf{h}_{1,LIN}+\mathbf{e} \quad [6]$$

where the design matrix $\mathbf{X}_1$ is the same as that used for Volterra analysis and $\mathbf{h}_{1,LIN}$ denotes the linear estimate of the hemodynamic response function (HRF). As discussed above, for experimental designs in which the stimuli are widely spaced such that there are no nonlinear interactions between the responses to different stimuli, the first order kernel $\mathbf{h}_1$ and the linear estimate $\mathbf{h}_{1,LIN}$ are equivalent. However, for designs in which the stimuli are closely spaced, such as those used in this study, the linear estimate $\mathbf{h}_{1,LIN}$ will not provide an accurate estimate of the HRF in the presence of nonlinearities. Thus, we expect that (1) the first order kernel $\mathbf{h}_1$ and the linear estimate $\mathbf{h}_{1,LIN}$ will differ when nonlinearities are present and (2) these differences will decrease as the system becomes more linear. To test this hypothesis, we also computed the linear estimates $\mathbf{h}_{1,LIN}$ from the average mixed response data.

Results

The top row of Figure 1 shows estimates of the first and second Volterra kernels for a representative subject. The first order kernel estimates from the pre-dose (blue) and post-dose (green) sessions are shown in panel (a), while the pre-dose and post-dose second order estimates are shown in panels (b) and (c), respectively. As described in the Methods section and Table 1, the kernel-based metrics of linearity (k_1, k_2, and k_∞) are the ratios of the norm of the first order kernel divided by the norm of the second order kernel, where the subscript on the metric

denotes the type of norm that is used. For this subject, the values of these metrics in the pre-dose session were k_1 =0.33, k_2 =1.00, and k_∞=2.60. In the post-dose session, the overall amplitude of the first order kernel is approximately the same as that of the pre-dose kernel, whereas the amplitude of the coefficients in the post-dose second order kernel (panel c) are visibly decreased as compared to the pre-dose kernel (panel b). As a result, the value of the linearity metrics are increased in the post-dose session, with values of k_1 =0.48, k_2 =1.83, and k_∞=6.57.

Representative linear (green) and nonlinear (dotted red) responses used to compute the additional linearity metrics are shown in the bottom two rows of Figure 1. Also shown is the full response (blue), which is the sum of the linear and nonlinear responses. Note that the nonlinear response is identically zero in the first 45 seconds, because there are no nonlinear interactions between the responses to the two period single trial stimuli presented in that time period. (As discussed in the Methods section, with the binary stimulus used in this study, we cannot uniquely identify the nonlinear response associated with a single stimulus). Consistent with the nonlinear response being identical to zero, the linear and full responses are equal to each other during the first 45 seconds. This initial 45 second period is therefore excluded from the computation of the linearity metrics. The values of the linearity metrics obtained from the ratio of the norms of the linear and nonlinear responses were l_1 =1.57 and l_2 =1.59 in the pre-dose condition and l_1 =2.05 and l_2 =1.96. This increase of the linearity metrics with caffeine is consistent with the reduction in the relative “size” of the nonlinear response in the post-dose session as compared to the pre-dose session. As the nonlinear response size decreases, the correlation coefficient between the linear and full responses increases, with a value of $r_{LIN,FULL}$ =0.82 in the pre-dose session and $r_{LIN,FULL}$ =0.91 in the post-dose session.

Scatter plots comparing the pre-dose and post-dose linearity metrics across the study sample are shown in Figure 2. The p-values and t-statistics obtained with two-tailed paired t-tests are indicated in each plot. For the kernel-based metrics (k_1, k_2, and k_∞) shown in the top row, the post-dose metrics were all significantly higher than the pre-dose metrics ($p< 0.02$). Similarly, for the response-based metrics (l_1, l_2, and $r_{LIN,FULL}$) shown in the bottom row, linearity was significantly increased ($p< 0.003$) in the post-dose session. Consistent with prior studies (Cameron et al. 1990;Field et al. 2003;Liu et al. 2004;Chen and Parrish 2009), caffeine led to a significant decrease in baseline CBF ($p = 0.0008$; $t(10) = -4.8$), with average pre-dose and post-dose values of 67 ml/(100g-min) and 46 ml/(100g-min), respectively.

As the BOLD dynamic response becomes more linear, estimates of the hemodynamic response functions (HRF) obtained assuming linearity ($\mathbf{h}_{1,LIN}$) are expected to become more similar to the Volterra kernel estimates of the impulse response ($\mathbf{h}_1$). Figure 3 shows the group average HRF estimates obtained using both linear analysis (red) and Volterra kernel analysis (blue) in the pre-dose (top row) and post-dose (bottom row) sessions. The HRFs are normalized by their maximum value to facilitate comparison of the shapes of the responses. From a qualitative viewpoint, the linear and Volterra-based HRF estimates show better agreement in the post-dose condition as compared to the pre-dose condition. For a quantitative comparison, we computed the correlation coefficients between the linear and Volterra-based HRF estimates. The post-dose correlation coefficients were significantly higher ($p = 0.013$, $t(10) = 3.03$) than the pre-dose values, with average values of 0.92 and 0.76, respectively.

Discussion

We have used a Volterra kernel analysis approach to show that the linearity of the visual BOLD response increases with the administration of caffeine. This finding is especially relevant for fMRI studies that utilize rapid event-related designs in which a linear analysis that ignores non-linearities can result in errors in estimates of the hemodynamic response function (Wager et

al. 2005). As the BOLD response becomes more linear, these errors will tend to diminish and the validity of estimates obtained with a linear analysis approach will increase.

Because caffeine affects both the neural and vascular systems, its effect on BOLD response linearity may reflect a combination of changes in both these systems. Vasoconstriction due to caffeine is thought to primarily reflect the antagonism of adenosine A_2 receptors (Fredholm et al. 1999). As discussed in the Introduction, prior work suggests that vasoconstriction may place the vascular system into a more linear region of operation (Kashikura et al. 2000; Kemna and Posse 2001; Cohen et al. 2002; Liu et al. 2004; Behzadi and Liu 2005; Behzadi and Liu 2006). In brief, as the smooth muscle in the vessel wall constricts due to the presence of a vasoconstrictive agent, the nonlinear effects of non-elastic connective tissue are decreased. The observed increase in BOLD response linearity with caffeine may therefore reflect the greater linearity of the vascular system. However, it is important to note that our results do not provide definitive evidence that vasoconstriction causes the change in linearity, and there may be other important mechanisms. For example, it is possible that the gain in linearity may also reflect the increase in baseline deoxyhemoglobin content that occurs with caffeine-induced vasoconstriction (Sedlacik et al. 2008). With increased deoxyhemoglobin, the BOLD signal can be less sensitive to nonlinear saturation effects, such as those observed in experiments where vasodilation due to either hypercapnia or acetazolamide reduces both the baseline deoxyhemoglobin content and the BOLD signal (Buxton et al. 2004). Further studies using other vasoconstrictive agents, as well as vasodilatory agents, would be useful for fully characterizing the relation between the baseline vascular state and the linearity of the BOLD response.

In addition to its vasoconstrictive effects, caffeine acts as a neurostimulant and directly influences neural activity by antagonizing adenosine A_1 receptors throughout the brain (Fredholm et al. 1999). Electroencephalographic (EEG) studies using a caffeine dose similar to that used in this study have reported caffeine-related increases in the task-related evoked responses (Pollock et al. 1981; Barry et al. 2007). However, there do not appear to be any studies that have examined the effect of caffeine on the dynamics of the task-related neural response. Nonlinear refractory effects in the neural response have been observed when brief stimuli are presented in close succession (e.g. less than 1 second intervals) (Ogawa et al. 2000). If these refractory effects depend on the amplitude of the evoked response, than it is conceivable that they could be affected by caffeine. Since neural systems tend to become more nonlinear as the size of the input increases (Wilson 1999), it is reasonable to conjecture that an increase in the evoked response with caffeine would tend to increase the nonlinear refractory effects, contrary to the findings of this study. Additional studies are needed to test this conjecture and directly assess the effect of caffeine on the linearity of the neural response.

It is also possible that the observed increase in linearity may have been affected by factors other than the direct vascular or neural effects of the caffeine dose, such as increased subject fatigue in the post-dose session or the psychological effects associated with a drug dose. As our protocol design did not employ a control session, we cannot completely rule out these other factors. Prior studies reporting an effect of caffeine on the BOLD signal have either used a protocol similar to that of the present study (Liu et al. 2004; Behzadi and Liu 2006) or have employed a control session (Mulderink et al. 2002; Liau et al. 2008; Perthen et al. 2008; Chen and Parrish 2009; Rack-Gomer et al. 2009). For studies that used a control session, no significant differences between the pre-dose and post-dose measures have been reported. Thus, it seems unlikely that the increase in linearity found in this study was primarily due to factors unrelated to the direct effects of the caffeine dose.

In this study, we adopted a Volterra kernel approach (Friston et al. 1998; Liu et al. 2002) to characterize the linearity of the BOLD response. Alternative approaches have been previously

used to assess the linearity of the BOLD response. One popular approach is to measure the responses to stimuli of varying durations and to then use the short duration responses to predict the long duration responses (Boynton et al. 1996; Vasquez and Noll 1998; Glover 1999; Birn et al. 2001; Liu and Gao 2001; Miller et al. 2001). In the presence of non-linearities, the predictions tend to overestimate the measured response. In another approach, the response to a series of pulses (typically two pulses) separated by varying intervals is measured (Friston et al. 1998; Huettel and McCarthy 2000; Ogawa et al. 2000; Yang et al. 2000). In the presence of nonlinear refractory effects, the response to the second pulse shows a reduction in amplitude as compared to what would be predicted from a linear time invariant model. As compared to these other approaches, the Volterra kernel approach has the advantage of providing kernel estimates that completely characterize the nonlinearities (up to second order) of the BOLD response. These kernel estimates can be used to predict the response to a wide variety of experimental designs, such as the varied duration and two-pulse designs. The Volterra kernel approach also has the advantage of being well suited for the analysis of rapid event-related designs in which the intervals between stimuli are determined by a random distribution. As these randomized designs are much more frequently used in practice than the varying duration or two-pulse designs, conclusions based on these designs are more readily applicable to a broader range of fMRI studies.

In summary, we found that caffeine significantly increased the linearity of the visual BOLD signal. Caffeine usage should be carefully considered in the analysis of rapid event-related fMRI experiments, especially for the vast majority of studies that assume linearity of the BOLD response. For these studies, differences in caffeine usage can lead to systematic biases in the linearity of the BOLD response and linear estimates of the hemodynamic response function. In addition, fMRI studies in which the baseline vascular state is modulated by disease or medication may also need to consider the extent to which the linearity of the BOLD response is altered by vasoconstrictive or vasodilatory factors. The dependence of hemodynamic response estimates on the linearity of the BOLD response is likely to vary with brain region, the type of stimulus used, and the specific stimulus timing employed in the experimental design. Because of this variation, it is difficult to make general predictions regarding the effect that changes in linearity, due to factors such as caffeine, will have on hemodynamic response estimates. As a result, it is recommended that investigators compute both linear and nonlinear estimates of the hemodynamic response function when there is reason to believe that there is a significant difference in linearity between groups or conditions.

Acknowledgments

We thank Yashar Behzadi, Joanna Perthen, Anna Leigh Rack-Gomer, and Khaled Restom for their assistance with this study. This work was funded by a Biomedical Engineering Research Grant from the Whitaker Foundation and by NIH Grant R01NS051661.

References

Barry RJ, Johnstone SJ, Clarke AR, Rushby JA, Brown CR, McKenzie DN. Caffeine effects on ERPs and performance in an auditory Go/NoGo task. Clin Neurophysiol 2007;118(12):2692–2699. [PubMed: 17905651]

Behzadi Y, Liu TT. An arteriolar compliance model of the cerebral blood flow response to neural stimulus. Neuroimage 2005;25(4):1100–1111. [PubMed: 15850728]

Behzadi Y, Liu TT. Caffeine reduces the initial dip in the visual BOLD response at 3 Tesla. NeuroImage 2006;32:9–15. [PubMed: 16635577]

Birn RM, Saad ZS, Bandettini PA. Spatial Heterogeneity of the Nonlinear Dynamics in the FMRI BOLD Response. NeuroImage 2001;14:817–826. [PubMed: 11554800]

Boynton GM, Engel SA, Glover GH, Heeger DJ. Linear systems analysis of functional magnetic resonance imaging in human V1. J. Neuroscience 1996;16:4207–4221.

Buckner RL, Snyder AZ, Sanders AL, Raichle ME, Morris JC. Functional brain imaging of young, nondemented, and demented older adults. J Cogn Neurosci 2000;12:24–34. [PubMed: 11506645]

Buxton RB, Uludag K, Dubowitz DJ, Liu TT. Modeling the hemodynamic response to brain activation. Neuroimage 2004;23:S220–S233. [PubMed: 15501093]

Cameron OG, Modell JG, Hariharan M. Caffeine and human cerebral blood flow: a positron emission tomography study. Life Sci 1990;47(13):1141–1146. [PubMed: 2122148]

Chalela JA, Alsop DC, Gonzalez-Atavales JB, Maldjian JA, Kasner SE, Detre JA. Magnetic resonance perfusion imaging in acute ischemic stroke using continuous arterial spin labeling. Stroke 2000;31(3): 680–687. [PubMed: 10700504]

Chen Y, Parrish TB. Caffeine dose effect on activation-induced BOLD and CBF responses. NeuroImage 2009;46(3):577–583. [PubMed: 19289172]

Cohen ER, Ugurbil K, Kim SG. Effect of basal conditions on the magnitude and dynamics of the blood oxygenation level-dependent fMRI response. J Cereb Blood Flow Metab 2002;22(9):1042–1053. [PubMed: 12218410]

Cox RW. AFNI-software for analysis and visualization of functional magnetic resonance neuroimages. Comput. Biomed. Res 1996;29:162–173. [PubMed: 8812068]

D'Esposito M, Zarahn E, Aguirre GK, Rypma B. The effect of normal aging on the coupling of neural activity to the BOLD hemodynamic response. NeuroImage 1999;10:6–14. [PubMed: 10385577]

Dale AM, Buckner RL. Selective averaging of rapidly presented individual trials using fMRI. Hum. Brain Mapp 1997;5:329–340.

Doyle, FJ.; Pearson, RK.; Ogunnaike, BA. Identification and Control Using Volterra Models. London: Springer-Verlag; 2002.

Farkas E, Luiten PG. Cerebral microvascular pathology in aging and Alzheimer's disease. Prog Neurobiol 2001;64(6):575–611. [PubMed: 11311463]

Field AS, Laurienti PM, Yen Y-F, Burdette JH, Moody DM. Dietary Caffeine Consumption and Withdrawal: Confounding Variables in Quantitative Cerebral Perfusion Studies? Radiology 2003;227:129–135. [PubMed: 12616005]

Forman SD, Cohen JD, Fitzgerald M, Eddy WP, Mintun MA, Noll DC. Improved assessment of significant activation in functional magnetic resonance imaging (fMRI): use of a cluster–size threshold. Magn. Reson. Med 1995;33:636–647. [PubMed: 7596267]

Fredholm BB, Battig K, Holmen J, Nehlig A, Zvartau EE. Actions of caffeine in the brain with special reference to factors that contribute to its widespread use. Pharmacol Rev 1999;51(1):83–133. [PubMed: 10049999]

Friston KJ, Josephs O, Rees G, Turner R. Nonlinear event-related responses in fMRI. Magn. Res. Med 1998;39:41–52.

Glover GH. Deconvolution of Impulse Response in Event-Related BOLD fMRI. NeuroImage 1999;9:416–429. [PubMed: 10191170]

Glover GH, Li TQ, Ress D. Image-based method for retrospective correction of physiological motion effects in fMRI: RETROICOR. Magn Reson Med 2000;44(1):162–167. [PubMed: 10893535]

Golub, GH.; Loan, CFV. Matrix Computations. Baltimore, Maryland: The Johns Hopkins University Press; 1989.

Hesselmann V, Zaro Weber O, Wedekind C, Krings T, Schulte O, Kugel H, Krug B, Klug N, Lackner KJ. Age related signal decrease in functional magnetic resonance imaging during motor stimulation in humans. Neurosci Lett 2001;308(3):141–144. [PubMed: 11479008]

Huettel SA, McCarthy G. Evidence for a Refractory Period in the Hemodynamic Response to Visual Stimuli as Meausured by MRI. NeuroImage 2000;11:547–553. [PubMed: 10806040]

Huettel SA, Singerman JD, McCarthy G. The effects of aging upon the hemodynamic response measured by functional MRI. Neuroimage 2001;13(1):161–175. [PubMed: 11133319]

Izzard AS, Rizzoni D, Agabiti-Rosei E, Heagerty AM. Small artery structure and hypertension: adaptive changes and target organ damage. J Hypertens 2005;23(2):247–250. [PubMed: 15662208]

Kashikura K, Kershaw J, Kashikura A, Matsuura T, Kanno I. Hyperoxia-enhanced activation-induced hemodynamic response in human VI: an fMRI study. Neuroreport 2000;11(5):903–906. [PubMed: 10790852]

Kemna LJ, Posse S. Effect of respiratory CO(2) changes on the temporal dynamics of the hemodynamic response in functional MR imaging. Neuroimage 2001;14(3):642–649. [PubMed: 11506537]

Liao D, Wong TY, Klein R, Jones D, Hubbard L, Sharrett AR. Relationship between carotid artery stiffness and retinal arteriolar narrowing in healthy middle-aged persons. Stroke 2004;35(4):837–842. [PubMed: 14988577]

Liau J, Liu TT. Inter-subject variability in hypercapnic normalization of the BOLD fMRI response. NeuroImage 2009;45(2):420–430. [PubMed: 19111622]

Liau J, Perthen JE, Liu TT. Caffeine reduces the activation extent and contrast-to-noise ratio of the functional cerebral blood flow response but not the BOLD response. Neuroimage 2008;42(1):296–305. [PubMed: 18514545]

Liu H-L, Gao J-H. An investigation of the impulse functions for the nonlinear BOLD response in functional MRI. Magn. Reson. Imaging 2001;18:931–938. [PubMed: 11121695]

Liu TT, Behzadi Y, Restom K, Uludag K, Lu K, Buracas GT, Dubowitz DJ, Buxton RB. Caffeine alters the temporal dynamics of the visual BOLD response. Neuroimage 2004;23(4):1402–1413. [PubMed: 15589104]

Liu, TT.; Buxton, RB.; Ghobrial, E. Unbiased Volterra Kernel Analysis of Event-Related fMRI Data. Proceedings of the 10th Meeting Intl. Soc. Magn. Reson. Med.; Honolulu, Hawaii. 2002. p. 752

Liu TT, Wong EC. A signal processing model for arterial spin labeling functional MRI. Neuroimage 2005;24(1):207–215. [PubMed: 15588612]

Mehagnoul-Schipper DJ, van der Kallen BF, Colier WN, van der Sluijs MC, van Erning LJ, Thijssen HO, Oeseburg B, Hoefnagels WH, Jansen RW. Simultaneous measurements of cerebral oxygenation changes during brain activation by near-infrared spectroscopy and functional magnetic resonance imaging in healthy young and elderly subjects. Hum Brain Mapp 2002;16(1):14–23. [PubMed: 11870923]

Miller KL, Luh WM, Liu TT, Martinez A, Obata T, Wong EC, Frank LR, Buxton RB. Nonlinear temporal dynamics of the cerebral blood flow response. Hum Brain Mapp 2001;13(1):1–12. [PubMed: 11284042]

Mulderink TA, Gitelman Dr, Mesulam M-M, Parrish TB. On the use of caffeine as a contrast booster for BOLD fMRI studies. NeuroImage 2002;15:37–44. [PubMed: 11771972]

Nowak RD, Van Veen BD. Random and Pseudorandom Inputs for Volterra Filter Identification. IEEE Trans. Signal proc 1994;42:2124–2135.

Ogawa S, Lee T-M, Stepnoski R, Chen W, Zhu X-H, Ugurbil K. An approach to probe some neural systems interaction by functional MRI at neural time scale down to milliseconds. Proc. Nat'l. Acad. Sci. USA 2000;97:11026–11031. [PubMed: 11005873]

Perthen JE, Lansing AE, Liau J, Liu TT, Buxton RB. Caffeine-induced uncoupling of cerebral blood flow and oxygen metabolism: a calibrated BOLD fMRI study. Neuroimage 2008;40(1):237–247. [PubMed: 18191583]

Pollock VE, Teasdale T, Stern J, Volavka J. Effects of caffeine on resting EEG and response to sine wave modulated light. Electroencephalogr Clin Neurophysiol 1981;51(5):470–476. [PubMed: 6165546]

Rack-Gomer AL, Liau J, Liu TT. Caffeine reduces resting-state BOLD functional connectivity in the motor cortex. NeuroImage 2009;46(1):56–63. [PubMed: 19457356]

Restom K, Behzadi Y, Liu TT. Physiological noise reduction for arterial spin labeling functional MRI. Neuroimage 2006;31(3):1104–1115. [PubMed: 16533609]

Richter W, Richter M. The shape of the fMRI BOLD response in children and adults changes systematically with age. Neuroimage 2003;20(2):1122–1131. [PubMed: 14568481]

Rosen BR, Buckner RL, Dale AM. Event-related functional MRI: Past, present, and future. Proc. Natl. Acad. Sci. USA 1998;95:773–780. [PubMed: 9448240]

Ross MH, Yurgelun-Todd DA, Renshaw PF, Maas LC, Mendelson JH, Mello NK, Cohen BM, Levin JM. Age-related reduction in functional MRI response to photic stimulation. Neurology 1997;48(1):173–176. [PubMed: 9008514]

Sedlacik J, Helm K, Rauscher A, Stadler J, Mentzel HJ, Reichenbach JR. Investigations on the effect of caffeine on cerebral venous vessel contrast by using susceptibility-weighted imaging (SWI) at 1.5, 3 and 7 T. NeuroImage 2008;40(1):11–18. [PubMed: 18226553]

Taoka T, et al. Age correlation of the time lag in signal change on EPI-fMRI. J Comput Assist Tomogr 1998;22(4):514–517. [PubMed: 9676437]

Vasquez AL, Noll DC. Nonlinear Aspects of the BOLD Response in Functional MRI. NeuroImage 1998;7:108–118. [PubMed: 9558643]

Wager TD, Vazquez A, Hernandez L, Noll DC. Accounting for nonlinear BOLD effects in fMRI: parameter estimates and a model for prediction in rapid event-related studies. Neuroimage 2005;25 (1):206–218. [PubMed: 15734356]

Wang J, Qiu M, Constable RT. In vivo method for correcting transmit/receive nonuniformities with phased array coils. Magn Reson Med 2005;53(3):666–674. [PubMed: 15723397]

Wilson, HR. Spikes, Decisions and Actions: Dynamical Foundations of Neuroscience. Oxford: Oxford University Press; 1999.

Wong EC, Buxton RB, Frank LR. Quantitative imaging of perfusion using a single subtraction (QUIPSS and QUIPSS II). Magn. Reson. Med 1998;39(5):702–708. [PubMed: 9581600]

Yang Y, Engelien W, Pan H, Xu S, Silbersweig DA, Stern E. A CBF-based event-related brain activation paradigm: Characterization of impulse-response function and comparison to BOLD. NeuroImage 2000;12:287–297. [PubMed: 10944411]

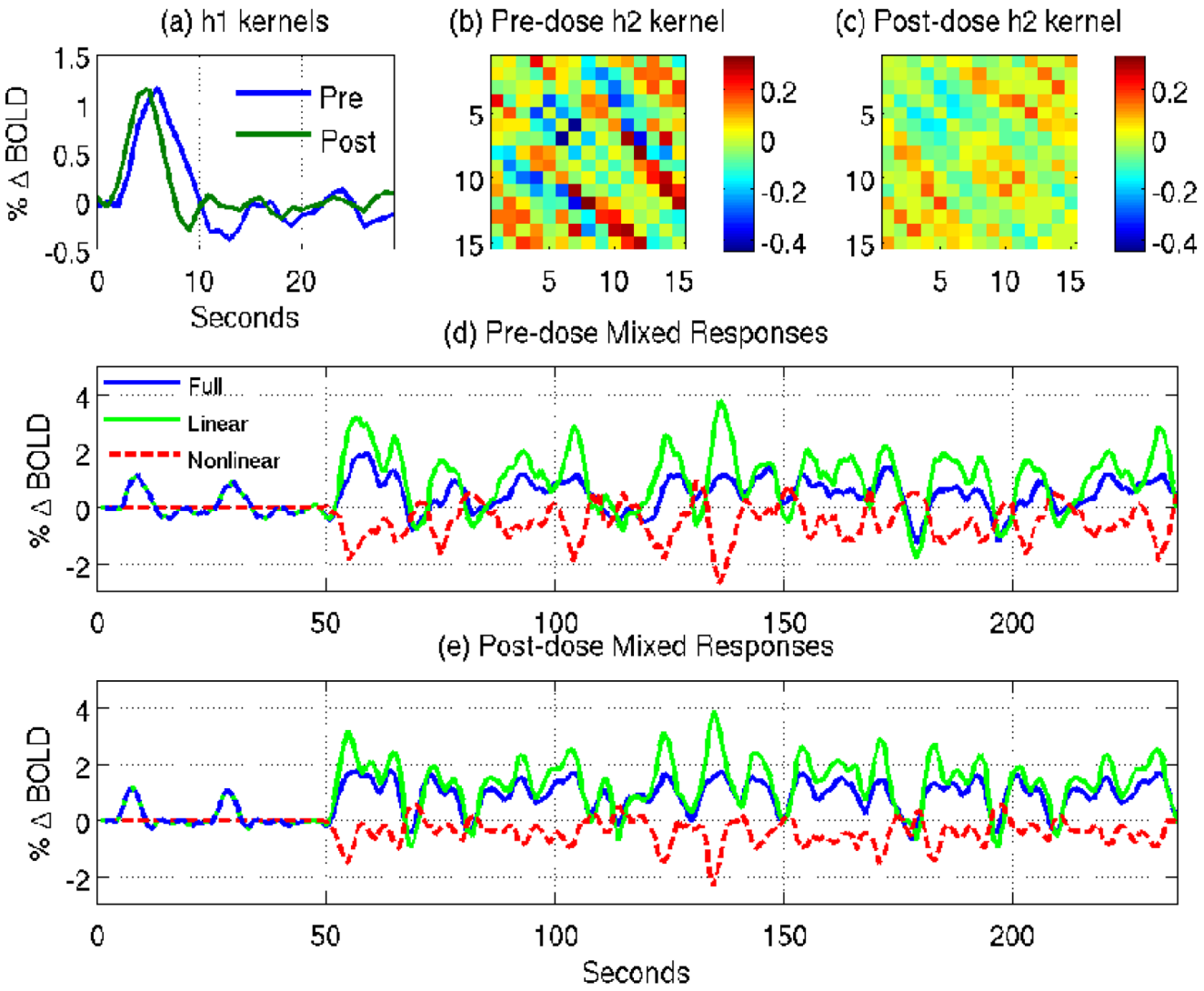

Figure 1.

Volterra kernel estimates and mixed response components from a representative subject. (a) Pre-dose (blue) and post-dose (green) first order kernel estimates. (b, c) Pre-dose and post-dose second order kernel estimates. The colorbar represents units of percent change BOLD signal. Axes of the kernels are in units of seconds. (d) Linear (green) and nonlinear (red) components of the pre-dose mixed response, as defined in Equations 3 and 4. The sum of these components is the full response (blue). (e) Linear, nonlinear, and full mixed responses for the post-dose condition. Note that the linear and full responses are equivalent during the first 45 seconds, because the nonlinear response is identically zero during this period (see Results section for additional discussion).

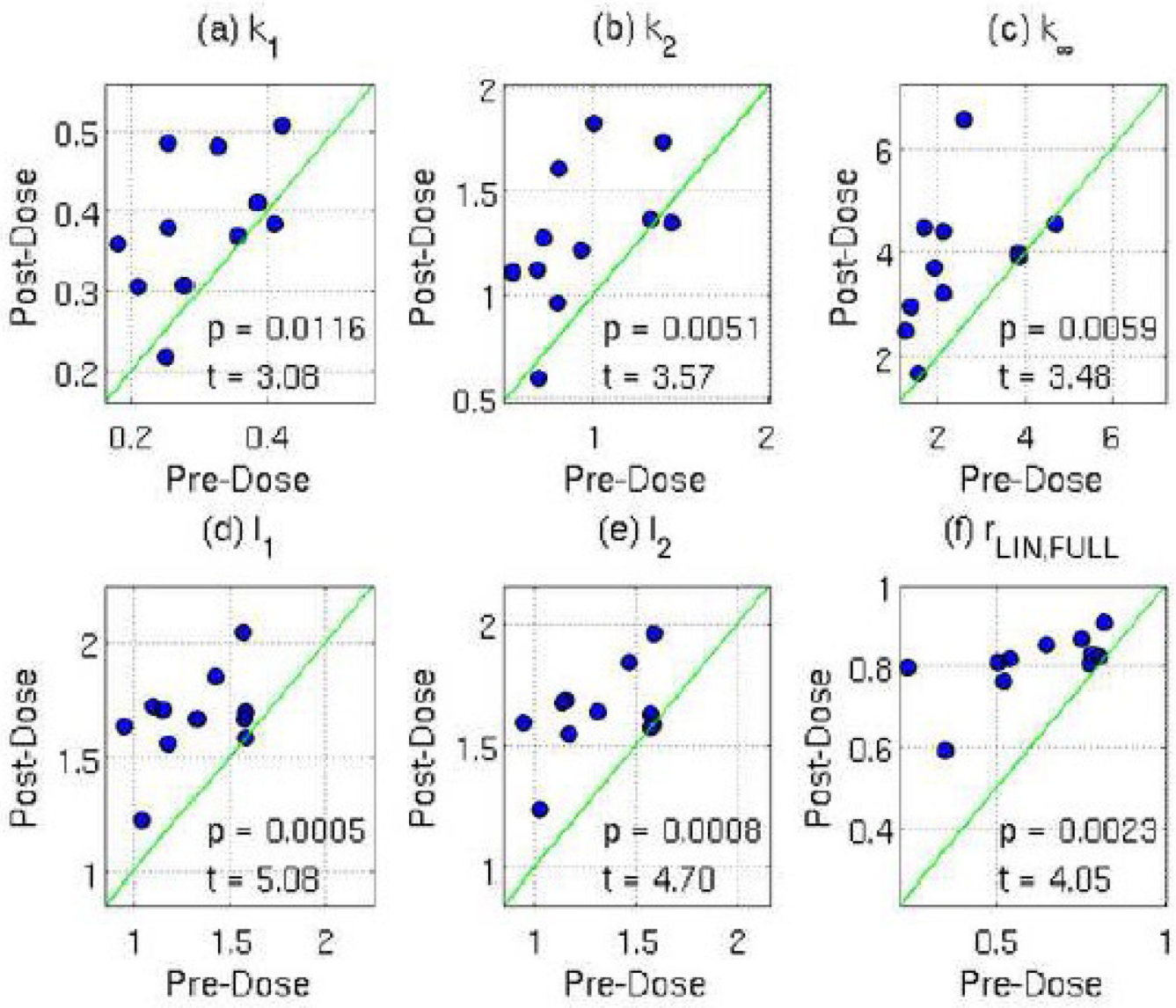

Figure 2.
Scatter plots of the post-dose versus pre-dose linearity metrics.

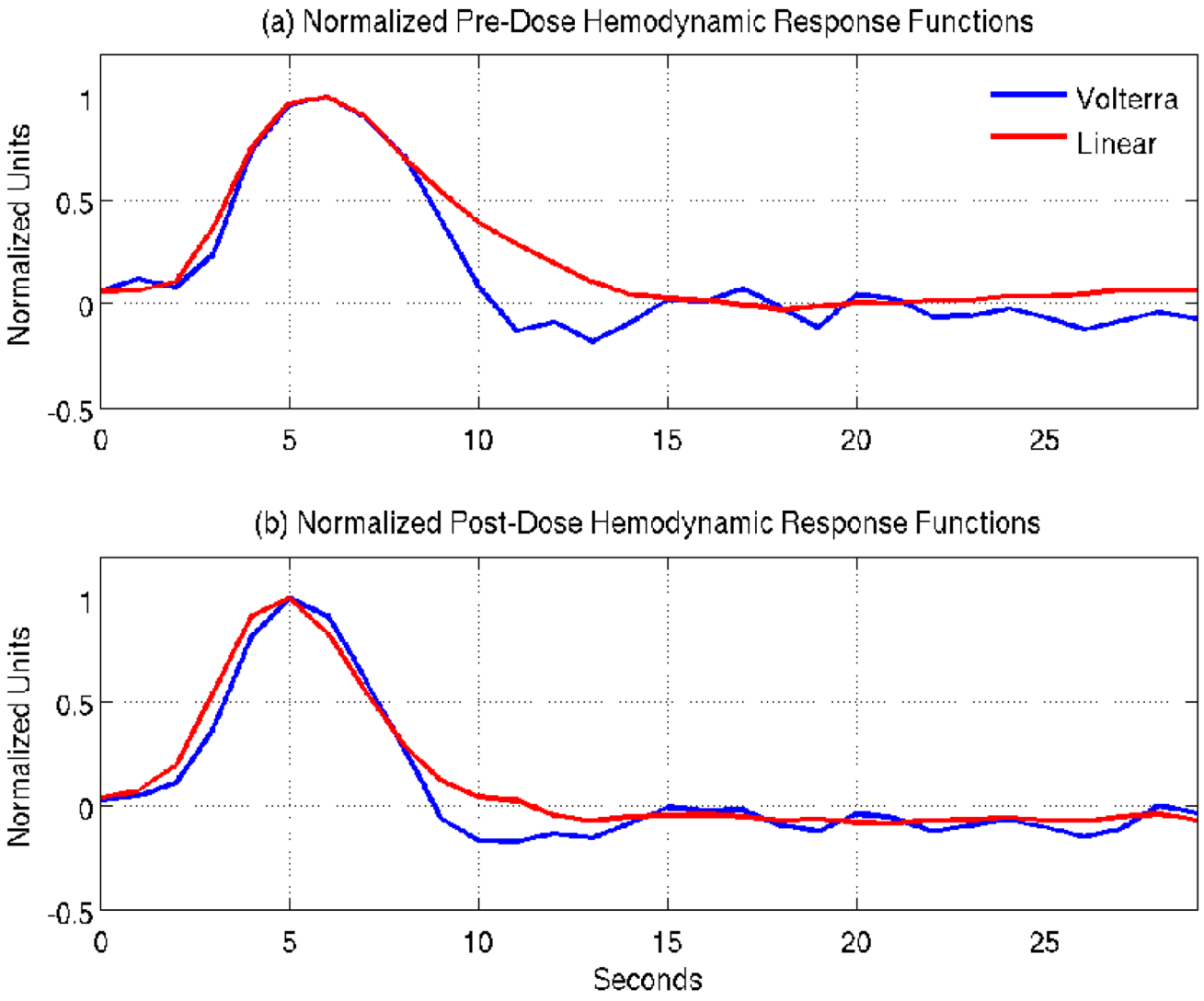

Figure 3.
Group average pre-dose (top) and post-dose (bottom) estimates of the hemodynamic response function. Estimates were obtained using Volterra kernel analysis (blue) and a linear analysis (red).

Table 1

Definitions of metrics of linearity.

Metrics of Linearity	Description
$k_1 = \frac{\|\mathbf{h}_1\|_1}{\|\mathbf{h}_2\|_1}$	Ratio of the L_1 norm of the linear kernel and second order kernels, where the L_1 norm is defined as the sum of the absolute values of the kernel elements.
$k_2 = \frac{\|\mathbf{h}_1\|_2}{\|\mathbf{h}_2\|_2}$	Ratio of the L_2 norms of the linear and second order kernels, where the L_2 norm is defined as the square root of the sum of squared values of the kernel elements.
$k_\infty = \frac{\max(\lvert\mathbf{h}_1\rvert)}{\max(\lvert\mathbf{h}_2\rvert)}$	Ratio of the maximum absolute values of the linear and second order kernels.
$l_1 = \frac{\|\mathbf{y}_{LIN} - \bar{\mathbf{y}}_{LIN}\|_1}{\|\mathbf{y}_{NONLIN} - \bar{\mathbf{y}}_{NONLIN}\|_1}$	Ratio of the L_1 norms of the linear and nonlinear components, after removal of the means.
$l_2 = \frac{\|\mathbf{y}_{LIN} - \bar{\mathbf{y}}_{LIN}\|_2}{\|\mathbf{y}_{NONLIN} - \bar{\mathbf{y}}_{NONLIN}\|_2}$	Ratio of the L_2 norms of the linear and nonlinear components, after removal of the means.
$r_{LIN,FULL} = corrcoef(\mathbf{y}_{LIN}, \mathbf{y}_{FULL})$	Correlation of the linear and full components.